

# Hadronic production of the $P$ -wave excited $B_c$ -states ( $B_{cJ,L=1}^*$ )

Chao-Hsi Chang<sup>1,2</sup> \*, Jian-Xiong Wang<sup>3†</sup> and Xing-Gang Wu<sup>3‡</sup>

<sup>1</sup>*CCAST (World Laboratory), P.O.Box 8730, Beijing 100080, China.*<sup>§</sup>

<sup>2</sup>*Institute of Theoretical Physics, Chinese Academy of Sciences,  
P.O.Box 2735, Beijing 100080, China.*

<sup>3</sup>*Institute of High Energy Physics, P.O.Box 918(4), Beijing 100039, China*

## Abstract

Adopting the complete  $\alpha_s^4$  approach of the perturbative QCD (pQCD) and updated parton distribution functions, we have estimated the hadronic production of  $P$ -wave excited  $B_c$ -states ( $B_{cJ,L=1}^*$ ). In the estimate, special care on the relation of the production amplitude to the derivative of wave function at origin of the potential model is paid. For experimental references, main uncertainties are discussed, and the total cross sections and the distributions of the production with reasonable cuts at the energies of Tevatron and LHC are computed and presented. The results show that  $P$ -wave production may contribute to the  $B_c$ -meson production indirectly by a factor about 0.5 of the direct production, and with such a big cross section, it is worth further to study the possibility to observe the  $P$ -wave production itself experimentally.

**PACS numbers:** 12.38.Bx, 13.85.Ni, 14.40.Nd, 14.40.Lb.

**Keywords:** inclusive hadronic production, excited  $B_c$  meson,  $P$ -wave states.

---

\* email: zhangzx@itp.ac.cn

† email: jxwang@mail.ihep.ac.cn

‡ email: wuxg@mail.ihep.ac.cn

§ Not correspondence address.

## I. INTRODUCTION

$B_c$  meson has been observed experimentally [1, 2], and the observations are in consistency with the theoretical prediction. In addition to the experimental progress, as theoretical studies of the meson  $B_c$  are getting deeply and widely [3, 4, 5, 6, 7, 8, 9, 10, 11, 12, 13, 14, 15, 16, 17, 18], recently  $B_c$  physics is attracting more and more attentions. For instance, considering the usages for experimental feasibility studies, we have written a generator named BCVEGPY [19] for the hadronic production of  $B_c$  ( $S$ -wave), which is a Fortran program package and is in PYTHIA format [20].

Since excited states of  $B_c$ , such as the  $P$ -wave states  $B_c^*(^1P_1)$  and  $B_c^*(^3P_J)(J = 1, 2, 3)$  (for shortening, hereafter we use the symbol  $B_{cJ,L=1}^*$  to denote these four  $P$ -wave states) etc, may directly or indirectly (cascade way) decay to the ground state with almost 100% possibility via electromagnetic or hadronic interactions, thus the production of the excited  $B_c$  states can be an additional source of the  $B_c$  mesons, i.e. the meson is produced in hadron collisions ‘indirectly’ but promptly. If one cannot discriminate the indirect  $B_c$  production and the direct one experimentally, but would like to try to well-understand the production of the meson  $B_c$ , one needs to know the indirect production fraction precisely. If one can discriminate the indirect  $B_c$  production and the direct one and, furthermore, the excited  $B_c$  states can be measured via their decay products exclusively experimentally i.e. the properties of the excited states will be measurable, and the potential models will have tests [12], the knowledge about the production certainly is very help for the experimental studies. Therefore, no matter the excited  $B_c$  states can be measured exclusively or not, the knowledge of the production of the excited states is requested. As known, to understand the hadronic production of  $J/\psi$  has a long story, even now there still are some problems e.g. experimental data still indicate not to agree with the theoretical prediction on the polarization of the hadronic produced  $J/\psi$  as well as the discrepancies of the  $J/\psi$  production in the B factory. While  $B_c$  is flavored explicitly, so not only its hadronic production but also its excited states’ hadronic production are simpler in comparison with those of the hidden flavored ( $c\bar{c}$ ) system. To understand hadronic production not only is needed for understanding ( $c\bar{b}$ )-quarkonium production, but also will help to clarify up the situation about the hadronic hidden heavy flavor ( $c\bar{c}$ ) production. To start with the  $P$ -wave excited state, to study the production and to write the generator accordingly are certainly interesting.

However, so far of the excited  $B_c$  states, only few authors of Refs.[21, 22, 23] have studied the hadronic production of the  $P$ -wave ones  $B_{cJ,L=1}^*$ . In Ref.[21], the hadronic  $B_{cJ,L=1}^*$  production has been calculated with the fragmentation approach, which is comparatively simple and can reach to the leading logarithm (LL) level of pQCD. But it seems that the approach can reach to a high accuracy only when the transverse momentum ( $p_t$ ) of  $B_c$  in the production is in very high region ( $p_t \gg 25$  GeV[9]). Alternatively, the complete  $\alpha_s^4$  approach has the great advantage that it retains the information about the  $\bar{c}$  and  $b$  quark (jets) associated with the  $B_{cJ,L=1}^*$  meson in the production although it is the lowest order (LO) pQCD calculation. From the experimental point of view to retain the information about the  $\bar{c}$  and  $b$  quark jets is more relevant. Therefore we would like to adopt the complete  $\alpha_s^4$  approach to study the  $P$ -wave production of the  $B_c$  excited states.

The amplitude for the  $P$ -wave state production involves the derivative of the wave function, so the derivation for the estimate is more complicated than the case of the  $S$ -wave state production. In fact, in the existence calculations in terms of the  $\alpha_s^4$  full amplitude approach [22, 23], the ‘derivative’ for the  $P$ -wave production is done numerically. To remind here, let us outline the situation for the two approaches to the hadronic production of  $B_{cJ,L=1}^*$ : the authors of Ref.[21] studied the production in terms of fragmentation approach, however, the authors of Ref.[22] pointed out that, similar to (even worse than) the  $S$ -wave case [8, 9], the results from fragmentation approach can be compared with those from the  $\alpha_s^4$  full amplitude approach only in the region where the transverse momentum of  $B_{cJ,L=1}^*$ ,  $p_t$ , is so high as  $p_t \geq 30$  GeV [22], and the total cross-section is much greater than that predicted by the fragmentation approach.

Since the results obtained by the above two approaches are not well consistent with each other, and considering the calculations are very complicated and the authors of Ref.[22] do the derivative numerically, thus we would like to re-calculate the production in terms of the  $\alpha_s^4$  full amplitude approach and pay great attention on the amplitude for the production how to relate to the derivative of the wave function at original. In certain sense, it is also to establish the relation between the matrix element appearing in nonrelativistic QCD [24] and the derivative of the wave function at original obtained in potential model precisely. We hope that we may clarify up the situation. We treat the hard subprocess amplitude in a strict way, that the first derivative, which is needed for  $P$ -wave production, over the relative momentum between the constituent quarks is done analytically and then we simplify the

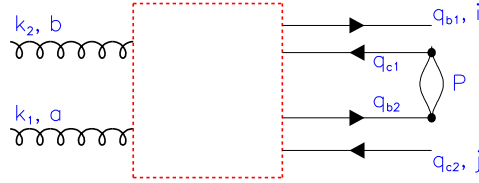


FIG. 1: The schematic diagram for the hadronic production of  $B_{cJ,L=1}^*$ , where the dashed box stands for the hard interaction kernel.  $k_1$  and  $k_2$  are two momenta for the initial gluons,  $q_{b1}$  and  $q_{c2}$  are the momenta for the outgoing  $b$  and  $\bar{c}$ ,  $P$  is the momentum of  $B_{cJ,L=1}^*$ .  $i, j, a$  and  $b$  are the color indexes of  $b, \bar{c}$  and the corresponding gluons.

amplitude of the hard subprocess amplitude analytically as possible as we can (including to find independent basic fermion strings and to expand the terms corresponding to Feynman diagrams accordingly etc) so that before the amplitude to be squared and the numerical calculations, we obtain a very condense formula for the amplitude. To guarantee the rightness of our calculations, we has done the check of the gauge invariance for the amplitude and with the same parameters to compare the results with the ones in Refs.[22, 23].

The paper is organized: to follow Introduction, in Sec.II we highlight the dominant mechanism of gluon-gluon fusion, and present the basic formula for the  $B_{cJ,L=1}^*$  hadronic production in the complete  $\alpha_s^4$  approach. In Sec.III, we describe the input parameters for numerical calculations and present the results properly. Finally, in Sec.IV we present discussions and a short summary.

## II. FORMULATION AND TECHNIQUE

Based on the factorization theorem of perturbative QCD (pQCD), the relevant hard subprocess plays a key role for hadronic production. In hadron collisions at high energies, for the production of the meson  $B_c$  and its excited states, the gluon-gluon fusion subprocess  $gg \rightarrow B_c(B_{cJ,L=1}^*) + b + \bar{c}$  is dominant [3, 4, 6, 7, 8, 9, 10, 11]. All of the discussions and calculations in the paper are based on the gluon-gluon fusion subprocess.

At the lowest order of pQCD ( $\alpha_s^4$  order), there are 36 Feynman diagrams for the gluon-gluon fusion process  $gg \rightarrow B_{cJ,L=1}^* + b + \bar{c}$  totally, which can be schematically expressed as

FIG.1, so accordingly there are 36 terms in the production amplitude. As in Ref.[19], here we would like to establish the exact relation of each term of the amplitude to the wave function (derivative of the wave function at origin for  $P$ -wave production) of potential model (also the relation between the matrix element in non-relativistic QCD (NRQCD) framework[24] and the wave function in potential model framework), thus we start with the ‘rule’ in Ref.[25] to write down the explicit expression for the term of the amplitude corresponding to the  $k$ th Feynman diagram:

$$M_k^{[(2S+1)P_J, J_z]} = C_{k,ij}^{ab} \bar{u}(q_{b1}) i \int \frac{d^4 q}{(2\pi)^4} \left( \Gamma_{1k} \cdot \bar{\chi}^{[(2S+1)P_J, J_z]}(q) \cdot \Gamma_{2k} \right) v(q_{c2}), \quad (1)$$

where  $\bar{\chi}^{[(2S+1)P_J, J_z]}(q)$  is the Bethe-Salpeter (BS) wave function for the bound state of  $(c\bar{b})$  in  $(2S+1)P_J$ , where  $C_{k,ij}^{ab}$  is the color factor,  $i, j$  are the outgoing  $b$  and  $\bar{c}$  quarks’ color indexes and  $a, b$  are the color indexes of the initial two gluons respectively.  $\Gamma_{1k}$  stands for the structure of the  $k$ -th Feynman diagram that is between  $\bar{u}(q_{b1})$  and the BS wave function  $\bar{\chi}^{[(2S+1)P_J, J_z]}(q)$ , which includes the relative string of Dirac  $\gamma$  matrices and the corresponding scalar part of the propagators,  $\Gamma_{2k}$  stands for the similar structure between the BS wave function  $\bar{\chi}^{[(2S+1)P_J, J_z]}(q)$  and  $v(q_{c2})$ .  $q_{b1}$  and  $q_{c2}$  are the momenta for the outgoing  $b$  quark and  $\bar{c}$  antiquark. In the non-relativistic approximation, the BS wave function  $\bar{\chi}^{[(2S+1)P_J, J_z]}(q)$  can be written:

$$\begin{aligned} \bar{\chi}^{[(2S+1)P_J, J_z]}(q) &\simeq \sum_{S_z, \lambda, \lambda'} \frac{-\sqrt{M}}{4m_b m_c} \cdot \Psi(q) \cdot (\epsilon^\lambda \cdot q) \cdot \\ &(\hat{q}_{b2} - m_b) \cdot (\delta_{S,0} \delta_{S_z,0} \gamma_5 + \delta_{S,1} \delta_{S_z, \lambda'} \hat{\epsilon}^{\lambda'}) \cdot (\hat{q}_{c1} + m_c) \cdot \langle 1\lambda; S S_z | J J_z \rangle, \end{aligned} \quad (2)$$

where  $P \equiv P_{B_{cJ,L=1}^*}$ ,  $M \equiv m_{B_{cJ,L=1}^*} \simeq m_c + m_b$  are the momentum, the mass of  $B_{cJ,L=1}^*$  meson respectively (i.e. for shortening the notation, we adopt  $P$  and  $M$  to denote the momentum, the mass of  $B_{cJ,L=1}^*$  meson respectively) and  $q$  is the relative momentum between the two constituent quarks. Since  $q_{b2}$  and  $q_{c1}$  are the momenta of the  $\bar{b}$  and  $c$  quarks inside the  $B_{cJ,L=1}^*$ , so they relate to the total and relative momenta of the bound state:

$$q_{b2} = \alpha_1 P - q, \quad q_{c1} = \alpha_2 P + q, \quad \alpha_1 = \frac{m_b}{m_c + m_b}, \quad \alpha_2 = \frac{m_c}{m_c + m_b}. \quad (3)$$

For convenience in later usages, let us introduce

$$q_\perp^\mu \equiv q^\mu - q_\parallel^\mu, \quad q_\parallel^\mu \equiv \frac{(P \cdot q)}{M^2} P^\mu$$

and  $q_{\parallel} \equiv |q_{\parallel}^{\mu}|$ , hence accordingly we have  $d^4q = dq_{\parallel}d^3q_{\perp}$ . The polarization vectors

$$(\epsilon^{\lambda} \cdot P) = (\epsilon^{\lambda'} \cdot P) = 0, \quad \lambda, \lambda' = (1, 0, -1);$$

$\Psi(q)$  stands for the ‘ $P$ -wave scalar wave function’, and  $\langle 1\lambda; SS_z | JJ_z \rangle$  is the Clebsch-Gordon coefficient for L-S coupling. In the paper, we will use  $\hat{a}$  to denote the contraction between the Dirac  $\gamma$  matrix and a momentum or polarization vector  $a$ , i.e. we use  $\hat{a}$  instead of  $\not{a}$ . The spin structure of the BS wave function  $\bar{\chi}^{[(2S+1)P_J, J_z]}(q)$  defined in Eq.(2) is of the lowest order (up to  $\mathcal{O}(q)$ ) for the  $P$ -wave state production.

The  $P$ -wave scalar function  $\Psi(q)$  in Eq.(2), as a factor of BS wave function, relates to the derivative of the wave function at origin  $\psi'_0(0)$  in coordinate representation under the so-called instantaneous approximation [26] by the integration:

$$i \int \frac{dq_{\parallel} d^3q_{\perp}}{(2\pi)^4} q^{\alpha} \Psi(q) (\epsilon^{\lambda} \cdot q) = i \int \frac{d^3q_{\perp}}{(2\pi)^3} \tilde{q}_{\perp}^{\alpha} \phi\left(-\frac{q_{\perp}^2}{M^2}\right) (\epsilon^{\lambda} \cdot q_{\perp}) = i \epsilon^{\lambda \alpha} \psi'(0). \quad (4)$$

Here  $\tilde{q}_{\perp}$  is the unit vector  $\frac{q_{\perp}}{\sqrt{-q_{\perp}^2}}$ , and  $\phi(-\frac{q_{\perp}^2}{M^2})$  stands for the  $P$ -wave ‘scalar wave function’ in the sense of potential model (the two quarks, as components of the bound state, must be in a relative space-like distance, hence  $\phi$  should be a function of the variable  $\frac{q_{\perp}^2}{M^2}$ ). Substituting Eq.(3) into Eq.(2), we obtain

$$\begin{aligned} i \int \frac{dq_{\parallel}}{(2\pi)} \bar{\chi}^{[(2S+1)P_J, J_z]}(q) &\simeq \sum_{S_z, \lambda, \lambda'} \phi\left(-\frac{q_{\perp}^2}{M^2}\right) (\epsilon^{\lambda} \cdot q_{\perp}) \langle 1\lambda; SS_z | JJ_z \rangle \\ &\cdot \left\{ \frac{1}{2\sqrt{M}} (-\hat{P} + M) \cdot (\delta_{S,0} \delta_{S_z,0} \gamma_5 + \delta_{S,1} \delta_{S_z, \lambda'} \hat{\epsilon}^{\lambda'}) \right. \\ &- \left( \frac{\sqrt{M}}{4m_b m_c} \right) \cdot \left[ \alpha_2 \hat{q}_{\perp} (-\hat{P} + M) (\delta_{S,0} \delta_{S_z,0} \gamma_5 + \delta_{S,1} \delta_{S_z, \lambda'} \hat{\epsilon}^{\lambda'}) \right. \\ &\left. \left. + \alpha_1 (-\hat{P} + M) \cdot (\delta_{S,0} \delta_{S_z,0} \gamma_5 + \delta_{S,1} \delta_{S_z, \lambda'} \hat{\epsilon}^{\lambda'}) \hat{q}_{\perp} \right] + \mathcal{O}(q_{\perp}^2) \right\} \\ &= \sum_{S_z, \lambda, \lambda'} \phi\left(-\frac{q_{\perp}^2}{M^2}\right) (\epsilon^{\lambda} \cdot q_{\perp}) \langle 1\lambda; SS_z | JJ_z \rangle (A_{SS_z}^{\lambda'} + B_{SS_z}^{\lambda' \mu} q_{\perp \mu} \\ &+ \mathcal{O}(q_{\perp}^2)), \end{aligned} \quad (5)$$

where

$$\begin{aligned} A_{SS_z}^{\lambda'} &\equiv \frac{1}{2\sqrt{M}} (-\hat{P} + M) \cdot (\delta_{S,0} \delta_{\lambda',0} \gamma_5 + \delta_{S,1} \delta_{S_z, \lambda'} \hat{\epsilon}^{\lambda'}), \\ B_{SS_z}^{\lambda' \mu} &\equiv - \left( \frac{\sqrt{M}}{4m_b m_c} \right) \cdot \left[ \alpha_2 \gamma^{\mu} (-\hat{P} + M) \cdot (\delta_{S,0} \delta_{\lambda',0} \gamma_5 + \delta_{S,1} \delta_{S_z, \lambda'} \hat{\epsilon}^{\lambda'}) \right. \\ &\left. + \alpha_1 (-\hat{P} + M) \cdot (\delta_{S,0} \delta_{\lambda',0} \gamma_5 + \delta_{S,1} \delta_{S_z, \lambda'} \hat{\epsilon}^{\lambda'}) \gamma^{\mu} \right]. \end{aligned}$$

Note that at the lowest order relativistic approximation the terms proportional to  $B_{SS_z}^{\lambda'\mu}$  do not contribute to the production of the  $S$ -wave  $B_c(B_c^*)$  meson at all, however, to the production of the  $P$ -wave states  $B_{cJ,L=1}^*$ , they do contribute, so we have to keep the terms with care. To reach to the lowest order of the relativistic approximation, according to Eq.(1) the next step is to do the expansion of the  $\Gamma_{1k}$  and  $\Gamma_{2k}$  about  $q_\mu$  up to  $\mathcal{O}(q^2)$  for the  $P$ -wave production, i.e.

$$\Gamma_{1k} = \Gamma_{1k}^0 + \Gamma_{1k}^\mu \cdot q_\mu + \mathcal{O}(q^2), \quad \Gamma_{2k} = \Gamma_{2k}^0 + \Gamma_{2k}^\mu \cdot q_\mu + \mathcal{O}(q^2), \quad (6)$$

where  $\Gamma_{1k}^0$ ,  $\Gamma_{1k}^\mu$ ,  $\Gamma_{2k}^0$  and  $\Gamma_{2k}^\mu$  does not depend on  $q^\mu$  (or  $q_\mu$ ) at all. Substituting the above equations into Eq.(1) and carrying out the integration over  $d^4q = dq_{\parallel}d^3q_{\perp}$  with the help of Eq.(4), we obtain

$$M_k^{S,JJ_z} = C_{k,ij}^{ab} \psi'(0) \sum_{S_z, \lambda, \lambda'} \langle 1\lambda; SS_z | JJ_z \rangle \epsilon_\mu^\lambda \cdot \bar{u}_s(q_{b1}) \left( \Gamma_{1k}^\mu \cdot A_{SS_z}^{\lambda'} \cdot \Gamma_{2k}^0 + \Gamma_{1k}^0 \cdot A_{SS_z}^{\lambda'} \cdot \Gamma_{2k}^\mu + \Gamma_{1k}^0 \cdot B_{SS_z}^{\lambda'\mu} \cdot \Gamma_{2k}^0 \right) v_{s'}(q_{c2}). \quad (7)$$

For a specific  $P$ -wave state, summing over the explicit  $\lambda$  and  $\lambda'$  for the Clebsch-Gordon coefficients, Eq.(7) can be further simplified as

$$M_k^{S,JJ_z} = C^{2S+1P_J} \psi'(0) C_{k,ij}^{ab} \cdot \bar{u}(q_{b1}) \left( \Gamma_{1k}^\mu \cdot E_\mu^{[2S+1P_J]J_z} \cdot \Gamma_{2k}^0 + \Gamma_{1k}^0 \cdot E_\mu^{[2S+1P_J]J_z} \cdot \Gamma_{2k}^\mu + \Gamma_{1k}^0 \cdot F^{[2S+1P_J]J_z} \cdot \Gamma_{2k}^0 \right) v(q_{c2}), \quad (8)$$

where the overall factor  $C^{(2S+1)P_J}$  and the functions  $E_\mu^{[2S+1P_J]J_z}$  and  $F^{[2S+1P_J]J_z}$  are computed separately for different  $P$ -wave states  $B_{cJ,L=1}^*$ .

For  $^1P_1$  state,  $J = 1$ ,  $J_z = \lambda$  and  $S = 0$ , we obtain

$$E_\mu^{[1P_1]\lambda} = (-\hat{P} + M)\gamma_5 \epsilon_\mu^\lambda, \quad F^{[1P_1]\lambda} = \frac{-\hat{P}\hat{\epsilon}^\lambda\gamma_5 + M(\alpha_1 - \alpha_2)\hat{\epsilon}^\lambda\gamma_5}{2M\alpha_1\alpha_2}, \quad C^{1P_1} = \frac{1}{2\sqrt{M}\sqrt{N_c}}. \quad (9)$$

Here and hereafter an extra factor  $1/\sqrt{N_c}$  will be implicitly included due to the fact that the meson is in color-singlet state.

The coefficients for the  $^3P_J$  ( $J = 0, 1, 2$ ) states with  $S = 1$  can be obtained with the help of the relations [29, 30]:

$$\sum_{\lambda, \lambda'} \langle 1\lambda; 1\lambda' | 00 \rangle \epsilon_\mu^\lambda \epsilon_\nu^{\lambda'} = \sqrt{\frac{1}{3}} \left( \frac{P_\mu P_\nu}{P^2} - g_{\mu\nu} \right), \quad (J = 0), \quad (10)$$

$$\sum_{\lambda, \lambda'} \langle 1\lambda; 1\lambda' | 1J_z \rangle \epsilon_\mu^\lambda \epsilon_\nu^{\lambda'} = i\sqrt{\frac{1}{2}} \epsilon_{\mu\nu}^{\rho\varrho} \frac{P_\rho}{M} \epsilon_\varrho^{J_z}, \quad (J = 1, J_z = -1, 0, 1), \quad (11)$$

$$\sum_{\lambda, \lambda'} \langle 1\lambda; 1\lambda' | 2J_z \rangle \epsilon_\mu^\lambda \epsilon_\nu^{\lambda'} = \epsilon_{\mu\nu}^{J_z}, \quad (J = 2, J_z = -2, -1, 0, 1, 2), \quad (12)$$

and the polarization vector  $\epsilon_\mu^\lambda$  and tensor  $\epsilon_{\mu\nu}(J_z)$  obey the projection relations

$$\sum_\lambda \epsilon_\mu^\lambda \epsilon_\nu^\lambda = \left( \frac{P_\mu P_\nu}{P^2} - g_{\mu\nu} \right) \equiv \mathcal{P}_{\mu\nu}, \quad (13)$$

$$\sum_{J_z} \epsilon_{\mu\nu}^{J_z} \epsilon_{\rho\varrho}^{J_z} = \frac{1}{2} [\mathcal{P}_{\mu\rho} \mathcal{P}_{\nu\varrho} + \mathcal{P}_{\nu\rho} \mathcal{P}_{\mu\varrho}] - \frac{1}{3} \mathcal{P}_{\mu\nu} \mathcal{P}_{\rho\varrho}, \quad (14)$$

for  ${}^3P_0$  state ( $\lambda = 0$ ):

$$E_\mu^{[{}^3P_0]\lambda} = (-\hat{P} + M)(M\gamma_\mu + P_\mu), \quad F^{[{}^3P_0]\lambda} = -\frac{3[(\alpha_2 - \alpha_1)\hat{P} + M]}{2\alpha_1\alpha_2}, \quad C^{{}^3P_0} = \frac{1}{2\sqrt{3N_c}M^{3/2}}; \quad (15)$$

for  ${}^3P_1$  state ( $\lambda = -1, 0, 1$ ):

$$E_\mu^{[{}^3P_1]\lambda} = i(\hat{P} + M)\epsilon_\mu^{\rho\varrho\nu}\gamma_\rho P_\varrho \epsilon_\nu^\lambda, \quad F^{[{}^3P_1]\lambda} = -\frac{\hat{P}\hat{\epsilon}^\lambda\gamma_5 - M\hat{\epsilon}^\lambda\gamma_5}{\alpha_1\alpha_2}, \quad C^{{}^3P_1} = \frac{1}{2\sqrt{2N_c}M^{3/2}}. \quad (16)$$

Finally for  ${}^3P_2$  state ( $J_z = -2, -1, \dots, 2$ ):

$$E_\mu^{[{}^3P_2]J_z} = (-\hat{P} + M)\gamma_5\gamma_\nu \epsilon_{\mu\nu}^{J_z}, \quad F^{[{}^3P_2]J_z} = 0, \quad C^{{}^3P_2} = \frac{1}{2\sqrt{N_c}M}. \quad (17)$$

If one calculates cross sections of the production by summing all the 36 terms (corresponding to the Feynman diagrams), and then having the result squared directly, the squared amplitude will be too long to deal with, even in terms of computer, and is really time-consuming to reach to the final results for the cross sections. Instead of summing the terms directly, we adopt the FDC package[27] to generate the Fortran program for each term and develop a technique in FDC further. Namely we firstly establish a complete set of ‘basic spinor lines’, such as that they are constructed by the multiplication of Dirac  $\gamma$  matrixes in a certain way as  $\hat{p}_1\hat{p}_2\hat{p}_3\cdots$ , then we consider them as bases to expand every terms of the amplitude and sum up all the terms according to the expansion (the coefficients of the ‘bases’ are summed respectively). In this way, the amplitude and its square become quite condense, thus the efficiency for computing the amplitude squared is raised greatly.

In order to simplify the amplitude manipulation under Fortran program, it is better to adopting the linear polarizations instead of the circular ones because the linear ones are real numbers. Thus we do so, and for convenience we put the explicit form of the linear

polarization vector  $\epsilon_\mu$  and that of tensor  $\epsilon_{\mu\nu}$  in Appendix I, which are used in our calculations when summing up the final polarizations of  $B_{c,L+1}^*$ .

The color factors for the terms corresponding to the Feynman diagrams should be also treated correctly. For the gluon-gluon fusion subprocess, we choose the three independent color factors[37] as follows:

$$T_{ij}^{1,ab} = \frac{3\sqrt{26}}{26\sqrt{15}}(2(T^a T^b)_{ij} + 2(T^b T^a)_{ij} - 3\delta_{ij} Tr[T^a T^b]), \quad (18)$$

$$T_{ij}^{2,ab} = \frac{\sqrt{2}}{2\sqrt{429}}(-11(T^a T^b)_{ij} + 2(T^b T^a)_{ij} - 3\delta_{ij} Tr[T^a T^b]), \quad (19)$$

$$T_{ij}^{3,ab} = \frac{\sqrt{2}}{2\sqrt{33}}(-3(T^b T^a)_{ij} - \delta_{ij} Tr[T^a T^b]), \quad (20)$$

with the normalization:  $\sum_{a,b,i,j} (T_{ij}^{m,ab\dagger} T_{ij}^{n,ab}) = \delta^{mn}$  ( $m = 1, 2, 3$ ). All the color factors  $C_{k,ij}^{ab}$  in Eq.(1) can be expanded as the linear combination of these three independent color factors. Therefore the amplitude can be grouped into three terms by ‘color’,

$$M^{S,JJ_z} = \sum_{k=1,\dots,36} M_k^{S,JJ_z} = \sum_{m=1,2,3} (T_{ij}^{m,ab} M_m^{S,JJ_z}). \quad (21)$$

For various un-polarized cross sections of the subprocess (in given  $J$  and  $S$ ), we have the square of the amplitude:

$$|M^{S,J}|^2 = \sum_{J_z} |M^{S,JJ_z}|^2. \quad (22)$$

According to pQCD factorization theorem, the hadronic production cross section is formulated as

$$d\sigma = \sum_{ij} \int dx_1 \int dx_2 F_{H_1}^i(x_1, \mu_F^2) \times F_{H_2}^j(x_2, \mu_F^2) d\hat{\sigma}_{ij \rightarrow B_{c,J,L=1}^*} X(x_1, x_2, \mu_F^2, Q^2), \quad (23)$$

where  $F_{H_1}^i(x, \mu_F^2)$ ,  $F_{H_2}^j(x, \mu_F^2)$  are the parton distribution functions (PDFs) of the  $i$  and  $j$  partons in the hadrons  $H_1$ ,  $H_2$  respectively.  $Q^2$  is the ‘squared energy scale’ where renormalization for the subprocess is made and  $\mu_F^2$  is the ‘squared energy scale’ where the factorization about the PDFs and the hard subprocess is made. Usually at LO the factorization and ‘renormalization’ are carried out at the same energy i.e.  $\mu_F^2 = Q^2$ , thus later on we take  $\mu_F^2 = Q^2$  and define  $d\hat{\sigma}_{ij \rightarrow B_{c,J,L=1}^*} X(x_1, x_2, Q^2) \equiv d\hat{\sigma}_{ij \rightarrow B_{c,J,L=1}^*} X(x_1, x_2, \mu_F^2, Q^2)$  except one case when estimating the uncertainty from LO and ambiguity of the choices of  $\mu_F^2$  and  $Q^2$ .

Having all the above preparations, we base on Eq.(23) technically to write a program for numerically computing the hadronic production cross sections at various energies [31].

### III. NUMERICAL RESULTS

Before doing numerical calculations, we have done the necessary checks. First of all, we numerically check the gauge invariance. We find the gauge invariance is guaranteed at the used computer ability level for our formula and computer program to compute the amplitude. Then we further compute the cross sections numerically for the subprocess  $g + g \rightarrow B_{cJ,L=1}^* + b + \bar{c}$  with the input parameters as taken in Ref.[22], and the same numerical results as those in Ref.[22] are obtained (see TABLE I, Fig.2 also Ref.[22]). Thus, we confirm the results of Ref.[22] for the subprocess, and are quite sure the correctness of our formula and program.

We should note here that the approximation Eq.(2), which is also taken in Ref.[22] and is similar in the cases for  $(c\bar{c})$  and  $(b\bar{b})$ , the heavy flavor hidden systems, indicates that the equations  $P = q_{c1} + q_{b2}$ ,  $q_{c1}^2 = m_c^2$ ,  $q_{b2}^2 = m_b^2$  and  $P^2 = m_{B_{cJ,L=1}^*}^2$  must be satisfied simultaneously, furthermore, only when the equations are satisfied, the gauge invariance of the amplitude is guaranteed. Therefore, under the approximation, there are two possibilities: one is to take the same quark mass values in the  $P$ -wave and  $S$ -wave state production, but one have to ignore the mass difference between the  $P$ -wave and  $S$ -wave states i.e.  $m_{B_c} = m_{B_{cJ,L=1}^*}$ ; the other one is to consider the mass differences between the  $P$ -wave and  $S$ -wave states i.e.  $m_{B_c} \neq m_{B_{cJ,L=1}^*}$  in the  $P$ -wave production, but one have to take different mass values of  $c$  and  $b$  quarks from those in  $S$ -wave production accordingly. The authors of Ref.[22] took the later i.e. they took  $m_b = 5.0$  GeV,  $m_c = 1.7$  GeV for the  $P$ -wave state production in order to have a mass of  $B_{cJ,L=1}^*$  about 6.7 GeV, although they took  $m_{B_c} = 6.3$  GeV,  $m_c = 1.5$  GeV and  $m_b = 4.8$  GeV for  $S$ -wave production in the meantime. As known that the cross section of the jet production  $g + g \rightarrow c + \bar{b} + b + \bar{c}$  is quite sensitive to the chosen values of the masses  $m_b$ ,  $m_c$ , thus, we think that the jet production should not be affected by the differences for the  $P$ -wave and  $S$ -wave production, and in fact that is also the requirement for the NRQCD formulism, of the two possibilities which cannot be avoided under the approximation Eq.(2), the former, i.e. to take  $m_{B_{cJ,L=1}^*} = m_{B_c}$  and to keep the values of  $b$  and  $c$  quark masses to be the same as those for the  $S$ -wave production, should be more relevant comparatively. Hence, in the paper we carry out all numerical calculations always to take the ‘choice’: the mass values of  $c, b$ -quarks as  $m_c = 1.5$  GeV  $m_b = 4.9$  GeV, i.e., the same as those taken in  $S$ -wave production, so  $m_{B_{cJ,L=1}^*} = m_{B_c} = 6.4$  GeV, except

TABLE I: The total cross section for the hard subprocess  $g + g \rightarrow B_{cJ,L=1}^* + b + \bar{c}$  (gluon fusion into  $P$ -wave excited states  $B_{cJ,L=1}^*$ ) at different C.M. energies. The input parameters are taken as those used in Ref.[22]:  $m_b = 5.0\text{GeV}$ ,  $m_c = 1.7\text{GeV}$ ,  $M = 6.7\text{GeV}$  and the running  $\alpha_s$  is fixed to 0.2 *etc.*

C.M. energy (GeV)	20GeV	40GeV	60GeV	80GeV	100GeV	200GeV
$\sigma(^1P_1)(pb)$	0.184	0.743	0.657	0.538	0.439	0.195
$\sigma(^3P_0)(pb)$	0.367	0.207	0.175	0.141	0.114	0.0496
$\sigma(^3P_1)(pb)$	0.346	0.598	0.503	0.402	0.324	0.139
$\sigma(^3P_2)(pb)$	0.721	1.49	1.31	1.06	0.862	0.374

the case when showing the uncertainties from the two possible choices.

As pointed out in Ref.[32], there are quit a lot of uncertainty sources in the hadronic production for the  $S$ -wave  $B_c(B_c^*)$  meson, such as the variations about  $\alpha_s$ -running, the variations in choices of the factorization energy scale, the adopted PDFs in different versions and various input parameter values relating the bound state *etc.*. For instance for definiteness in check of our formula and computer program by comparison with the results of [22], we take pQCD coupling constant  $\alpha_s = 0.2$ , the derivative of the wave function at origin  $|R'(0)|^2 = 0.201\text{GeV}^5$ , and the mass values of  $c$ -quark,  $b$ -quarks and  $B_{cJ,L=1}^*$  are fixed as  $m_b = 5.0\text{GeV}$ ,  $m_c = 1.7\text{GeV}$ ,  $M = 6.7\text{GeV}$  *etc* i.e. all are fixed as those in [22] for the subprocess  $gg \rightarrow B_{cJ,L=1}^* + b + \bar{c}$ .

To compute the production, we need to know the PDFs. Several groups, such as CTEQ [33], GRV [34] and MRS [35] *etc.*, devote themselves to offer accurate PDFs to the world. By taking different PDFs, one may find that the results caused by different PDFs can be about 10%. Later on for definiteness, we will take CTEQ6L[33] and the leading order  $\alpha_s$  running with  $\Lambda_{QCD}^{(n_f=4)} = 0.326\text{ GeV}$ .

As pointed out in Ref.[32], at LO pQCD of all the uncertainties, that caused by the choice of the factorization energy scale  $Q^2$  for the hadronic production is the largest, and for  $S$ -wave production it may cause such uncertainty as great around a factor 30%. In fact, it is also the case. To see the uncertainty caused by  $Q^2$  choice for the  $P$ -wave production, we try to calculate the  $P$ -wave production with the other factors being fixed. As in Ref.[32] we

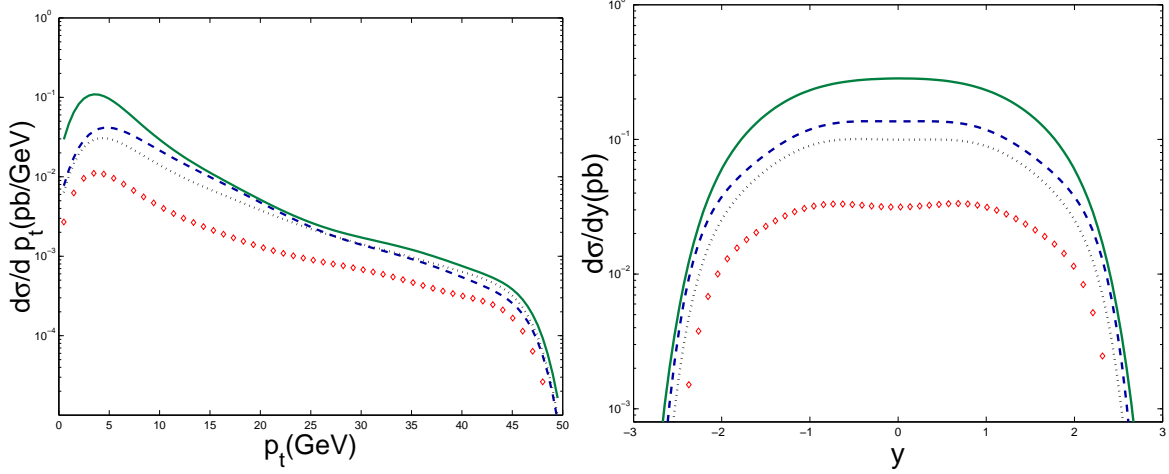


FIG. 2:  $B_{c,L=1}^* - p_t$  and  $B_{c,L=1}^* - y$  differential distributions for the subprocess. The dashed line (up-middle), the diamond line (bottom), the dotted line (down-middle) and the solid line (top) are for  $^1P_1$ ,  $^3P_0$ ,  $^3P_1$  and  $^3P_2$ , respectively. The parameters are taken to be the same ones that have been used in Ref.[22].

TABLE II: The total cross section (in unit nb) for the hadronic production of  $P$ -wave  $B_c$  meson ( $B_{c,J,L=1}^*$ ) at LHC and TEVATRON with different types of factorization energy scales ( $A, B, C, D$ ). Here  $m_b = 4.9$  GeV,  $m_c = 1.5$  GeV and  $m_{B_{c,J,L=1}^*} = m_c + m_b$ .

-	LHC ( $\sqrt{S} = 14.$ TeV)				TEVATRON ( $\sqrt{S} = 1.96$ TeV)			
	$A$	$B$	$C$	$D$	$A$	$B$	$C$	$D$
$\sigma(^1P_1)(nb)$	4.738	9.123	9.825	8.379	0.2555	0.6545	0.7547	0.5507
$\sigma(^3P_0)(nb)$	1.910	3.288	3.523	3.036	0.1161	0.2563	0.2966	0.2149
$\sigma(^3P_1)(nb)$	4.117	7.382	7.304	6.682	0.2289	0.5597	0.6490	0.4780
$\sigma(^3P_2)(nb)$	10.18	20.40	21.71	18.26	0.5096	1.350	1.515	1.102

take four types of  $Q^2$  choices and put the results for total cross section in Tab.II respectively.

The four types are:

Type  $A$ :  $Q^2 = \hat{s}$ , the squared C.M. energy of the subprocess;

Type  $B$ :  $Q^2 = M_t^2 \equiv p_t^2 + m_{B_{c,J,L=1}^*}^2$ , the squared transverse mass of the  $B_{c,J,L=1}^*$  meson;

Type  $C$ ,  $Q^2 = m_{bt}^2 \equiv p_{tb}^2 + m_b^2$ , the squared transverse mass of the  $b$  quark.

Type  $D$ :  $Q^2 = 4m_b^2$ .

From Tab.II about the total cross sections for the hadronic production of  $B_{c,J,L=1}^*$  at

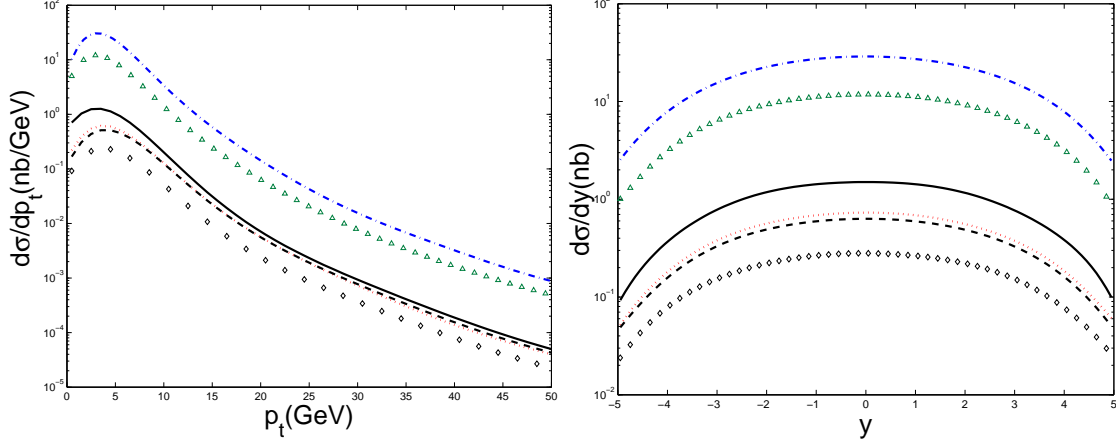


FIG. 3: The differential distributions of  $p_t$  and  $y$  for the hadronic production of  $B_{cJ,L=1}^*$  at LHC. The dotted line (down-middle), the diamond line (bottom), the dashed line (next to bottom), the solid line (up-middle) are for  $^1P_1$ ,  $^3P_0$ ,  $^3P_1$ ,  $^3P_2$ , respectively. For comparison, the results for  $^1S_0$  and  $^3S_1$  wave states are shown in triangle line (next to top) and dash-dot line (top) correspondingly (with parameters:  $m_b = 4.9$  GeV,  $m_c = 1.5$  GeV and  $m_{B_c} = m_{B_{cJ,L=1}^*} = m_c + m_b$ ).

LHC and TEVATRON with the different types of the choices, one may observe that the  $Q^2$  dependence in the  $P$ -wave  $B_{cJ,L=1}^*$  production is much more stronger than that in the  $S$ -wave production. With the different choices, the total cross sections of the production can be varied so big as a factor  $2.0 \sim 3.0$ .

For definiteness in the rest estimates on the production we will adopt just Type  $B$  for  $Q^2$  choice.

For experimental references, we also calculate the distributions of  $p_t$  and  $y$  (the  $B_{cJ,L=1}^*$  transverse momentum and rapidity) precisely and draw the curves on the distributions in Fig.3 for LHC and in Fig.4 for TEVATRON.

For comparison, in Figs.3,4, we also show the  $p_t$  and  $y$  differential distributions for the production of the  $S$ -wave states  $^1S_0$  and  $^3S_1$ . One may observe that the  $p_t$  and  $y$  dependence of the differential distributions behaves quite similar to those of the  $^1S_0$  state production. The summed up  $P$ -wave production cross section of the  $P$ -waves  $^1P_1, ^3P_0, ^3P_1, ^3P_2$  is smaller than the  $S$ -wave production, but it can reach to a fraction about 50% of the  $^1S_0$  production cross section.

From FIGs.3,4, one may also see that the  $p_t$  and  $y$  differential distributions for the hadronic production of  $B_{cJ,L=1}^*$  are quite different at LHC and at TEVATRON due to the

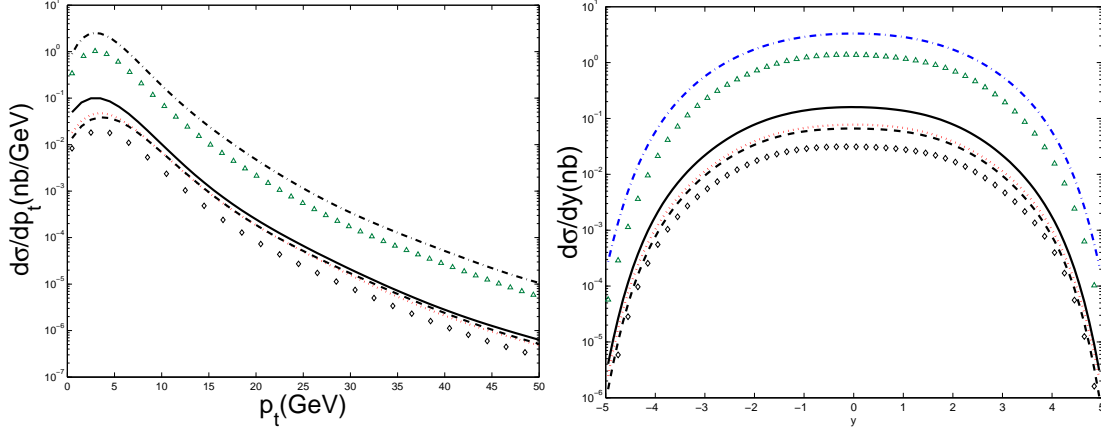


FIG. 4: The differential distributions of  $p_t$  and  $y$  for the hadronic production of  $B_{c,J,L=1}^*$  at TEVATRON. The dotted line (down-middle), the diamond line (bottom), the dashed line (next to bottom), the solid line (up-middle) are for  $^1P_1$ ,  $^3P_0$ ,  $^3P_1$ ,  $^3P_2$ , respectively. For comparison, the results for  $^1S_0$  and  $^3S_1$  wave states are shown in triangle line (next to top) and dash-dot line (top) correspondingly (with parameters:  $m_b = 4.9$  GeV,  $m_c = 1.5$  GeV and  $m_{B_c} = m_{B_{c,J,L=1}^*} = m_c + m_b$ ).

different C.M. energies of the two colliders.

To see the uncertainties from  $Q^2$  choice, instead of variation on the choices with  $Q^2 = \mu_F^2$ , the authors in literature, such as Ref.[36], also try  $Q^2 \neq \mu_F^2$  in Eq.(23) and see the uncertainty. Here following them, we calculate the summed  $p_t$ - and  $y$ -distributions of all the  $P$ -wave  $B_{c,L=1}$  production for LHC and TEVATRON and present the uncertainty on the distributions in FIGs.5,6 respectively. One may see the uncertainty can be so great as a factor 4.0.

In high energy hadronic colliders, the events with a small  $p_t$  and/or a large rapidity  $y$  cannot be detected by detectors directly, so for experimental studies and for precise purposes in the estimates, only the events with proper kinematic cuts on  $p_t$  and  $y$  are taken into account. In Ref.[32], we did the studies on the  $S$ -wave production, thus for experimental references here we also try various cuts for the  $P$ -wave production.

To study the cut effects on the production, here we consider the production in summing up all of the  $P$ -wave ( $^1P_0, ^3P_0, ^3P_1, ^3P_2$ ) production. Considering the abilities in measuring rapidity of  $B_c$  for the detectors CDF, D0 and BTeV at TEVATRON, and ATLAS, CMS and LHC-B at LHC, we try the rapidity cuts  $y_{cut} \sim 1.5$  and higher for  $p_t$  distribution and the  $p_{tcut} \sim 5$  GeV and higher for  $y$  distribution. The results with the four cuts:  $y_{cut} =$

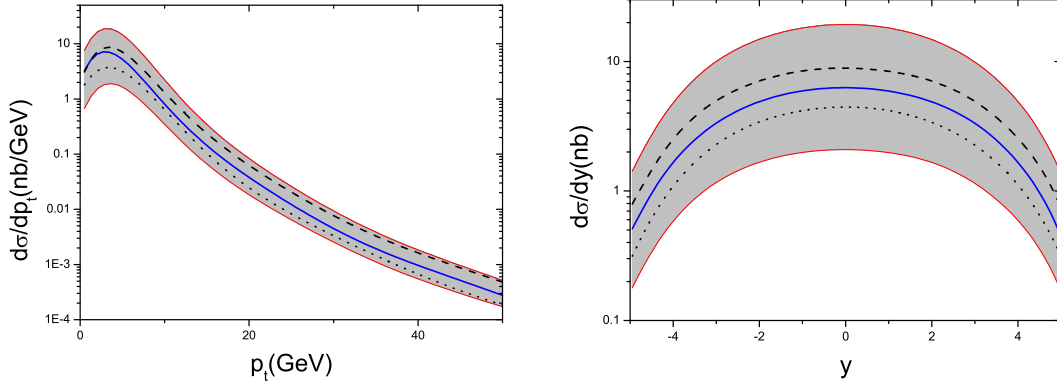


FIG. 5: The summed  $p_t$ - and  $y$ -distributions of all the  $P$ -wave  $B_{c,L=1}$  for different values of the factorization scale  $\mu_F^2$  and the renormalization scale  $Q^2$  at LHC. The upper edge of the band corresponds to  $\mu_F^2 = 4M_t^2$ ,  $Q^2 = M_t^2/4$  and the lower edge corresponds to that of  $\mu_F^2 = M_t^2/4$ ,  $Q^2 = 4M_t^2$ . The solid line, the dotted line and the dashed line corresponds to that of  $\mu_F^2 = Q^2 = M_t^2$ ,  $\mu_F^2 = Q^2 = 4M_t^2$ ,  $\mu_F^2 = Q^2 = M_t^2/4$  respectively.

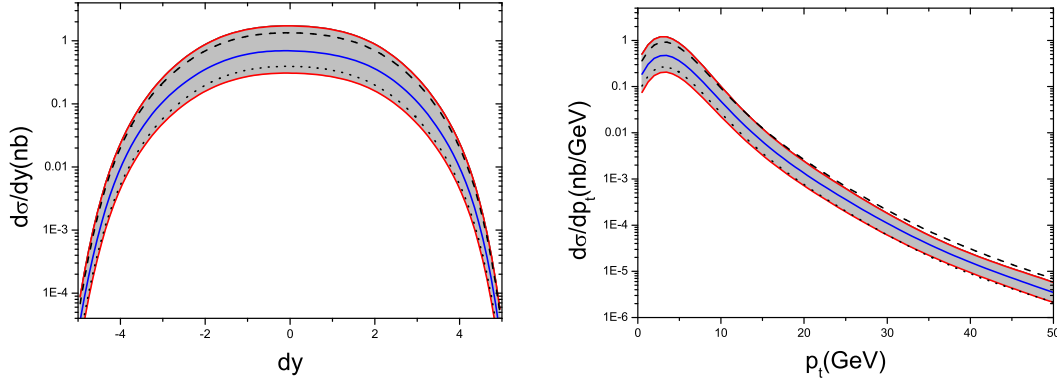


FIG. 6: The summed up  $p_t$ - and  $y$ -distributions of all the  $P$ -wave  $B_{c,L=1}$  for different values of the factorization scale  $\mu_F^2$  and the renormalization scale  $Q^2$  at TEVATRON. The upper edge of the band corresponds to  $\mu_F^2 = 4M_t^2$ ,  $Q^2 = M_t^2/4$  and the lower edge corresponds to that of  $\mu_F^2 = M_t^2/4$ ,  $Q^2 = 4M_t^2$ . The solid line, the dotted line and the dashed line corresponds to that of  $\mu_F^2 = Q^2 = M_t^2$ ,  $\mu_F^2 = Q^2 = 4M_t^2$ ,  $\mu_F^2 = Q^2 = M_t^2/4$  respectively.

(0.5, 1.0, 1.5, 2.0) are put in FIG.7 and the results with the four cuts:  $p_{tcut} = 5, 20, 35, 50$  GeV are put in FIG.8.

From Fig.7, we can see that the dependence of the  $p_t$  distributions on  $y_{tcut}$  for LHC

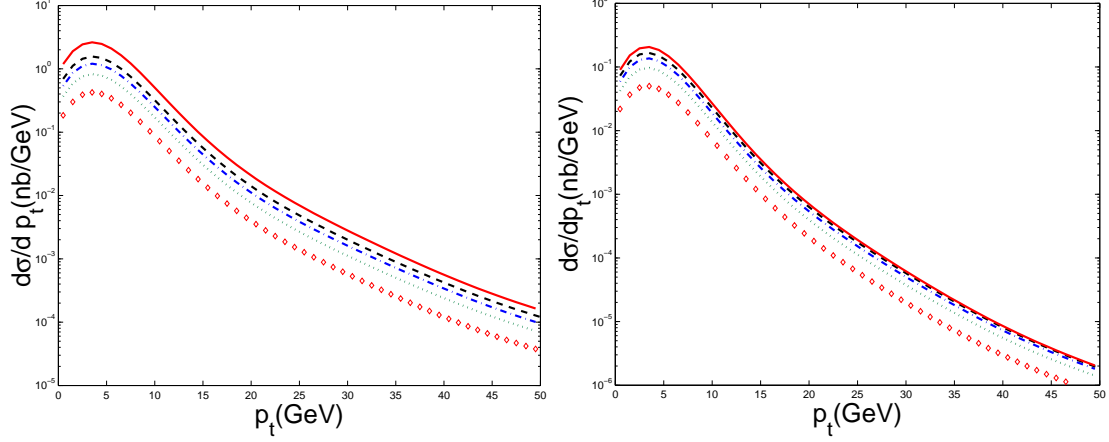


FIG. 7: The summed up differential distributions for all the considered  $P$ -wave state production versus  $p_t$  of  $B_{cJ,L=1}^*$  with a  $y$  cut ( $y_{cut}$ ) at LHC (left) and at TEVATRON (right). Dashed line (next to top) with  $y_{cut} = 2.0$ ; dash-dot line (middle) with  $y_{cut} = 1.5$ ; dotted line (next bottom) with  $y_{cut} = 1.0$ ; diamond line (bottom) with  $y_{cut} = 0.5$  and solid line (top) without  $y_{cut}$ .

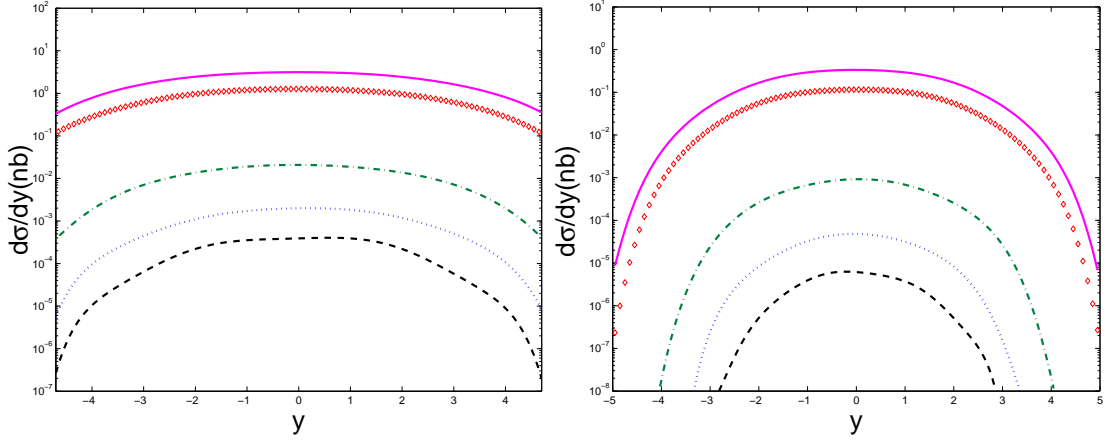


FIG. 8: The summed up differential distributions for all the considered  $P$ -wave state production versus rapidity  $y$  of  $B_{cJ,L=1}^*$  with a transverse momentum cut ( $p_{tcut}$ ) at LHC (left) and at TEVATRON (right). Diamond line (next to top) with  $p_{tcut} = 5$  GeV; dash-dot line (middle) with  $p_{tcut} = 20$  GeV; dotted line (next to bottom) with  $p_{tcut} = 35$  GeV; dashed line (bottom) with  $p_{tcut} = 50$  GeV and solid line (top) with  $p_{tcut} = 0$ .

is stronger than that for TEVATRON. This is because that at TEVATRON, the sizable rapidity distributions cover a smaller region in  $y$ , so generally speaking the rapidity cuts affect the production stronger than that at LHC. The correlations between  $p_t$  and  $y$  can be seen more clearly from Fig.8, the  $y$ -distribution various  $p_t$ -cuts. One may observe that the

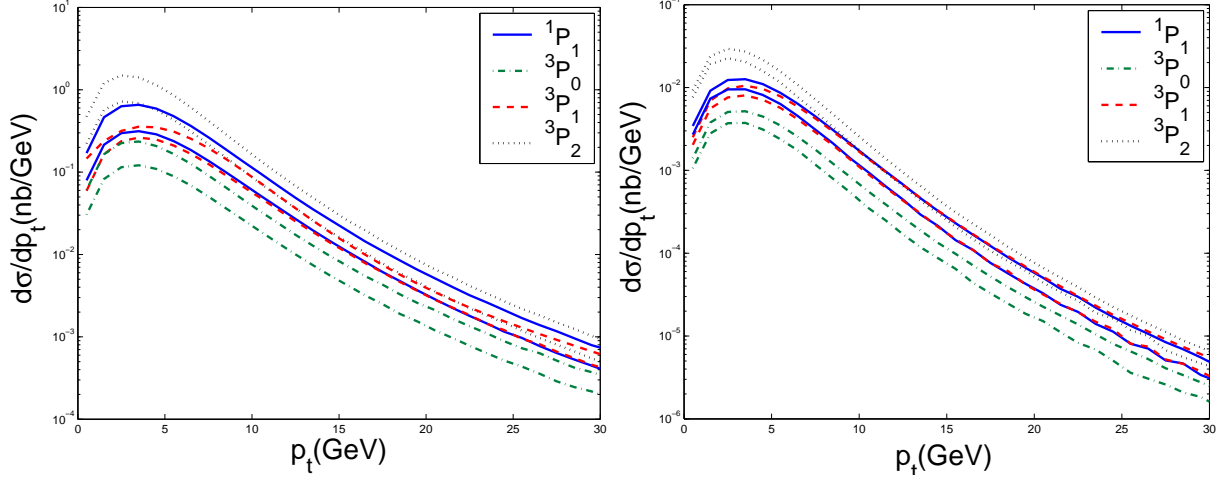


FIG. 9: The  $p_t$  distributions of all the  $P$ -wave  $B_{c,L=1}^*$  ( $^1P_1$  and  $^3P_J$  ( $J = 1, 2, 3$ )) production at LHC (left) and TEVATRON (right). Of the same type of lines, the upper is for the choice:  $m_b = 4.9$  GeV,  $m_c = 1.5$  GeV, while the lower is for the choice:  $m_b = 5.0$  GeV,  $m_c = 1.7$  GeV, respectively. For LHC, we take  $|y| \leq 1.5$  and for TEVATRON, we take  $|y| \leq 0.6$ .

dependence of the differential distribution on rapidity  $y$  with different  $p_{tcut}$  is to exhibit a broader profile at LHC than at TEVATRON.

We also would like specially to show the consequences due to the approximation Eq.(2) with one by the two possibilities described above, i.e. the one taken by ourselves:  $m_{B_{c,J,L=1}^*} = m_{B_c} = 6.4$  GeV,  $m_c = 1.5$  GeV and  $m_b = 4.9$  GeV, and the other one taken by Refs.[22, 23]:  $m_{B_{c,J,L=1}^*} = 6.7$  GeV,  $m_c = 1.7$  GeV and  $m_b = 5.0$  GeV quantitatively, because it is ‘fresh’ in  $P$ -wave production. We calculate  $p_t$  distributions for the  $P$ -wave ( $^1P_1, ^3P_0, ^3P_1, ^3P_2$ ) production with the two possibilities respectively and draw the curves of the differential cross sections versus  $p_t$  in FIG.9. It is obvious that with our present parameters for the constitute quarks, the distributions (hence the total cross-sections) are about two times bigger than that of the second choice for the constitute quark masses. Namely, the results mean that the consequences due to the approximation Eq.(2) are sizable and indicate improvement on the approximation is requested.

#### IV. DISCUSSIONS AND SUMMARY

In the paper, we have studied the hadronic production of the  $P$ -wave  $B_{cJ,L=1}^*$  in a way as analytical as possible, i.e., the amplitude of the hard subprocess  $g + g \rightarrow B_{c,L=1}^* + b + \bar{c}$  is reduced with the help of the FDC program [27] and the technique to expand each term of the amplitude by the independent ‘bases’ for the ‘elementary fermion strings’ analytically then to sum up all of the 36 terms (corresponding to the 36 Feynman diagrams). Thus having the amplitude in expansion of the bases squared, we have made the numerical calculations very efficiently. The correctness for the amplitude and the program is tested by demonstrating its gauge invariance numerically up to the computer abilities and comparing the results for the subprocess with those in Ref.[22] by taking the same parameters. Having done the tests, we will add the whole program into the  $B_c$  meson generator as the new version **BCVEGPY2.0** soon[31].

From the figures FIGs.2,3,4 and the tables Tabs.I,II, one may see that, of the hadronic  $P$ -wave production, that of  $^3P_2$  is the biggest and that of  $^3P_0$  is the smallest. From the table Tab.II and the figures FIGs.5,6, one may see that, at LO, the uncertainties from the factorization and renormalization energy scale choice, i.e. on  $Q^2, \mu_F^2$  choices for the  $P$ -wave production, are quite great, even greater than that of  $S$ -wave production. Furthermore, from the figure FIG.9, one may see that the approximation Eq.(2) causes a great uncertainty in the production estimate.

Relating to the approximation, our results with the choice  $m_{B_{cJ,L=1}^*} = m_{B_c} = 6.4$  GeV,  $m_c = 1.5$  GeV and  $m_b = 4.9$  GeV can be almost two times bigger than the results obtained in Ref.[22] with the choice  $m_{B_{cJ,L=1}^*} = 6.7$  GeV,  $m_c = 1.7$  GeV and  $m_b = 5.0$  GeV at LHC and TEVATRON. The fact about the factor 2 can be understandable: as known, smaller quark masses will cause the cross section of the four quark production  $gg \rightarrow c + \bar{c} + b + \bar{b}$  bigger and they will also cause an increase effect in the binding  $c + \bar{b} \rightarrow B_{cJ,L=1}^*$ , thus when we take smaller masses of quarks and also the bound state mass  $M = m_b + m_c$  in the meantime, we obtain such bigger results by the factor 2 than those in Ref.[22]. We think that for the production the true values (without the approximation Eq.(2) for a more accurate estimate) should be smaller than those we present here, due to a comparatively small value of the masses of  $B_{cJ,L=1}^*$  taken here, but the true values should be bigger than those obtained in Ref.[22] due to there comparatively big values for the masses of  $c$  and  $b$  quarks taken for

the factor of the four quark production inside the  $P$ -wave production respectively. Since the factor of the involved production  $gg \rightarrow b\bar{b}c\bar{c}$  is guaranteed in gauge invariance, here only the factor  $c\bar{b} \rightarrow B_{cJ,L=1}^*$  is not well treated in the present results, while in Ref.[22] not only the factor  $c\bar{b} \rightarrow B_{cJ,L=1}^*$  but also the factor of the involved four quark production are not well-treated by comparatively bigger values for the quarks and the bound states, so we suspect that the true values for the production might be closer to the presented ones here, rather than those in Ref.[22]. Note that the term  $B_{ss_z}^{\lambda \mu} q_\mu$  in Eq.(5) does not play any role for  $S$ -wave  $B_c$  and  $B_c^*$  production at all, thus for the  $S$ -wave production the approximate choices about the values of  $P = q_{c1} + q_{b2}$ ,  $m_c$ ,  $m_b$  and  $m_{B_c(B_c^*)}$  are not so sensitive as the  $P$ -wave production.

The summed total cross section for all of the considered hadronic  $P$ -wave production can be so big as a half of the direct production of the ground state  $B_c(1S_0)$ . Considering the the fact that almost all of the  $P$ -excited states  $B_c^*(3S_1)$  decay to the ground state  $B_c$ , the contribution from the  $B_c^*(3S_1)$  production to the ‘final  $B_c$ -wave production’, we may conclude that the contribution can be about 20% in total. From the  $p_t$  and  $y$  distributions, one may see that  $P$ -wave and  $S$ -wave production behave quite similar, that no matter what  $p_{tcut}$  and  $y_{cut}$  are chosen, the  $P$ -wave production itself with such big cross sections is worth while to study the possibility directly measuring the  $P$ -wave  $B_c$ -states seriously. Especially, the properties of the  $P$ -wave mesons  $B_{(c,L=1)}^*$  are crucial in understanding the mass spectrum of the  $c\bar{b}$ -quarkonium states and testing the potential models.

**Acknowledgements:** This work was supported in part by the Natural Science Foundation of China (NSFC).

- 
- [1] CDF Collaboration, F. Abe *et al.*, Phys. Rev. D **58**, 112004 (1998).
  - [2] D0 Collaboration,  $B_c$  and heavy baryon properties at D0 and CDF, presented by S. Towers in *ICHEP'04*, Aug.16-22, 2004, Beijing.
  - [3] K. Anikeev *et al.*, hep-ph/0201071.

- [4] Chao-Hsi Chang, Talk in *ATLAS Physics Workshop* 12-16 Sept. 2001, at Lund University; *Proceedings of the XXXVIIIth RENCONITRES DE MORIOND: 2002 QCD and High Energy Hadronic Interactions*, Les Arcs, Savoie, France, **p-27**, hep-ph/20205112.
- [5] C. Quigg, *Proceedings of the Workshop on B Physics at Hadron Accelerators*, Snowmass (CO) USA, 1993, Eds. P. McBride and C.S. Mishra.
- [6] Chao-Hsi Chang and Yu-Qi Chen, *Phys. Rev. D* **46**, 3854 (1992); Erratum *Phys. Rev. D* **50**, 6013 (1994).
- [7] E. Braaten, K. Cheung and T.C. Yuan, *Phys. Rev. D* **48**, 4230 (1993); E. Braaten, K. Cheung and T.C. Yuan, *Phys. Rev. D* **48**, R5049 (1993).
- [8] Chao-Hsi Chang and Yu-Qi Chen, *Phys. Rev. D* **48**, 4086 (1993).
- [9] Chao-Hsi Chang, Yu-Qi Chen, Guo-Ping Han and Hung-Tao Jiang, *Phys. Lett. B* **364**, 78 (1995); Chao-Hsi Chang, Yu-Qi Chen and R. J. Oakes, *Phys. Rev. D* **54**, 4344 (1996); K. Kolodziej, A. Leike and R. Rückl, *Phys. Lett. B* **355**, 337 (1995).
- [10] A.V. Berezhnoy, V.V. Kiselev, A.K. Likhoded, *Z. Phys. A* **356**, 79 (1996); S.P. Baranov, *Phys. Rev. D* **56** 3046, (1997).
- [11] K. Cheung, *Phys. Lett. B* **472**, 408 (2000).
- [12] Yu-Qi Chen and Yu-Ping Kuang, *Phys. Rev. D* **46**, 1165 (1992); E. Eichten, C. Quigg, *Phys. Rev. D* **49** 5845 (1994); *Phys. Rev. D* **52**, 1726 (1995); S.S. Gershtein, V.V. Kiselev, A.K. Likhoded and A.V. Tkabladze, *Phys. Rev. D* **51**, 3613 (1995).
- [13] Chao-Hsi Chang, Yu-Qi Chen, *Phys. Rev. D* **49**, 3399 (1994); Chao-Hsi Chang and Yu-Qi Chen, *Commun. Theor. Phys.* **23** (1995) 451.
- [14] A. Abd El-Hady, J.H. Munoz and J.P. Vary, *Phys. Rev. D* **62** 014014 (2000).
- [15] N. Isgur, D. Scora, B. Grinstein and M. Wise, *Phys. Rev. D* **39**, 799 (1989); M. Lusignoli and M. Masetti, *Z. Phys. C* **51**, 549 (1991); D. Scora and N. Isgur, *Phys. Rev. D* **52**, 2783 (1995). Dongsheng Du, G.-R. Lu and Y.-D. Yang, *Phys. Lett. B* **387**, 187 (1996); Dongsheng Du *et al.*, *Phys. Lett. B* **414**, 130(1997); Jia-Fu Liu and Kuang-Ta Chao, *Phys. Rev. D* **56** 4133, (1997); P. Colangelo and F.De Fazio, *Phys. Rev. D* **61** 034012 (2000). V.V. Kiselev, A.E. Kovalsky and A.K. Likhoded, *Nucl. Phys. B* **585** 353 (2000); V.V. Kiselev, A.K. Likhoded and A.I. Onishchenko, *Nucl. Phys. B* **569** 473, (2000). M.A. Nobes and R.M. Woloshyn, *J. Phys. G* **26** 1079, (2001).
- [16] Chao-Hsi Chang, Shao-Long Chen, Tai-Fu Feng and Xue-Qian Li, *Phys. Rev. D* **64**, 014003

- (2001); Commun. Theor. Phys. **35**, 51 (2001).
- [17] M. Beneke and G. Buchalla, Phys. Rev. D **53**, 4991 (1996).
- [18] Chao-Hsi Chang, J.-P. Cheng and C.-D. Lü, Phys. Lett. B **425**, 166 (1998); P. Colangelo and F. De Fazio, Mod. Phys. Lett. A **14**, 2303 (1999); Chao-Hsi Chang, Cai-Dian Lü, Guo-Li Wang and Hong-Shi Zong, Phys. Rev. D **60** 114013, 1999; Chao-Hsi Chang, Yu-Qi Chen, Guo-Li Wang and Hong-Shi Zong, Phys. Rev. D **65**, 014017 (2001); Commun. Theor. Phys. **35**, 395 (2001); Chao-Hsi Chang, Anjan K. Giri, Rukmani Mohanta and Guo-Li Wang, J. Phys. G **28**, 1403, (2002), hep-ph/0204279; Xing-Gang Wu, Chao-Hsi Chang, Yu-Qi Chen and Zheng-Yun Fang, Phys. Rev. D **67**, 0704XX, (2003), hep-ph/0209125.
- [19] Chao-Hsi Chang, Chafik Driouich, Paula Eerola and Xing-Gang Wu, Comput. Phys. Commun. **159**, 192 (2004).
- [20] T. Sjostrand, Comput. Phys. Commun. **82**, 74 (1994).
- [21] K.M. Cheung and T.C. Yuan, hep-ph/9409353.
- [22] A.V. Berezhnoy, V.V. Kiselev and A.K. Likhoded, Phys. Atom. Nucl. **60**, 100 (1997); Yad. Fiz. **60**, 108 (1997).
- [23] A.V. Berezhnoy, V.V. Kiselev and A.K. Likhoded, Z.Phys. A**356**, 79(1996); A.V. Berezhnoi, V.V. Kiselev, A.K. Likhoded and A.I. Onishchenko, Phys.Atom.Nucl. **60**, 1729 (1997).
- [24] Geoffrey T. Bodwin, Eric Braaten and G. Peter Lepage, Phys. Rev. D **51**, 1125 (1995); Erratum Phys. Rev. D **55**, 5853 (1997).
- [25] S. Mandelstam, Proc. R. Soc. London **233**, 248(1955). Likhoded, Z. Phys. A **356**, 79(1996); Chao-Hsi Chang, Tso-Hsiu Ho and Tao Huang, *Physica Acta*, **25**, 215 (1976) (in Chinese).
- [26] E.E. Salpeter, Phys. Rev. **87**, 328 (1952).
- [27] Jian-Xong Wang, FDC *New computing techniques in physics research* Proceedings of AI93, Oberamergan, Germany, III 517-522; *Progress in FDC project* hep-ph/0407058.
- [28] Chao-Hsi Chang, Yu-Qi Chen, Guo-Li Wang and Hong-Shi Zong, Phys. Rev. D **65**, 014017(2002).
- [29] G. Guberina, J.H. Kuhn, R.D. Peccei and R. Ruckl, Nucl. Phys. B **174**, 317(1980).
- [30] Y.Q. Chen, Phys. Rev. D **48**, 5181(1993).
- [31] Chao-Hsi Chang, J.X. Wang and X.G. Wu, an improved version for BCVEGPY1.0 is in preparation.
- [32] Chao-Hsi Chang and X.G. Wu, to appear in Eur. Phys. J. C, hep-ph/0309121.

- [33] H.L. Lai, et al., hep-ph/0201195.
- [34] M. Glueck, E. Reya, A. Vogt, Eur. Phys. J. C **5**, 461(1998).
- [35] A.D. Martin, R.G. Roberts, W.J. Stirling and R.S. Thorne, Eur. Phys. J. C **23**, 73(2002).
- [36] M. Klasen, B.A. Kniehl, L.N. Mihaila and M. Steihauser, Phys. Rev. Lett. **89**, 032001(2002).
- [37] In Refs.[8, 9], the number  $N$  for color group is considered as a variable, so it is to conclude that there are 5 independent color factors there. While here  $N$  is fixed to be equal to 3, thus there are three independent color factor only.

## APPENDIX A: THE LINEAR POLARIZATION VECTOR AND TENSOR

As stated in the text, the linear polarization vector (tensor) contains real number only if the meson (bound state) is a vector (tensor) meson, so the linear ones are better than complex circular polarization ones in numerical calculations, thus the linear explicit expressions for them are quite useful in writing numerical programs. Hence, we present the precise expressions for the linear polarization vector if the meson is a vector one, and the polarization tensor if the meson is a tensor one in the appendix.

We set a coordinate first, in which  $z$ -axial is in the direction of the incoming hadron, and the momentum of the concerned meson (bound state) in the direction:  $P^\mu = (P_0, |\vec{P}| \sin \theta \cos \phi, |\vec{P}| \sin \theta \sin \phi, |\vec{P}| \cos \theta)$  with  $|\vec{P}| = \sqrt{P_0^2 - M^2}$ , i.e.,  $\theta$  is the polar angle and  $\phi$  is the azimuth angle in the coordinate. The space-like linear polarization vector for the meson can be expressed as:

$$\epsilon_x^\mu(\vec{P}) : (0, \cos \theta \cos \phi, \cos \theta \sin \phi, -\sin \theta) \quad (\text{A1})$$

$$\epsilon_y^\mu(\vec{P}) : (0, -\sin \phi, \cos \phi, 0) \quad (\text{A2})$$

$$\epsilon_z^\mu(\vec{P}) : \frac{1}{M}(|\vec{P}|, P_0 \sin \theta \cos \phi, P_0 \sin \theta \sin \phi, P_0 \cos \theta). \quad (\text{A3})$$

As the request of the polarization vector definition, they do satisfy the conditions:

$$\epsilon_i \cdot P = 0, \quad \epsilon_i \cdot \epsilon_j = -\delta_{ij}, \quad (i, j = x, y, z). \quad (\text{A4})$$

Accordingly, the ‘linear polarization tensor’  $\epsilon_{J_z}^{\alpha\beta}(P)$  for  $B_c^*(^3P_2)$  can be constructed in the following way i.e. the five components ( $J_z = 1, 2, \dots, 5$ ) of the polarization tensor are constructed in terms of  $\epsilon_x(\vec{P})$ ,  $\epsilon_y(\vec{P})$  and  $\epsilon_z(\vec{P})$ :

$$\epsilon_1^{\mu\nu} = \frac{1}{\sqrt{2}}(\epsilon_x^\mu \epsilon_y^\nu + \epsilon_y^\mu \epsilon_x^\nu), \quad \epsilon_2^{\mu\nu} = \frac{1}{\sqrt{2}}(\epsilon_x^\mu \epsilon_z^\nu + \epsilon_z^\mu \epsilon_x^\nu),$$

$$\begin{aligned}
\epsilon_3^{\mu\nu} &= \frac{1}{\sqrt{2}}(\epsilon_y^\mu \epsilon_z^\nu + \epsilon_z^\mu \epsilon_y^\nu), & \epsilon_4^{\mu\nu} &= \frac{1}{\sqrt{2}}(\epsilon_x^\mu \epsilon_x^\nu - \epsilon_y^\mu \epsilon_y^\nu), \\
\epsilon_5^{\mu\nu} &= \frac{1}{\sqrt{6}}(\epsilon_x^\mu \epsilon_x^\nu + \epsilon_y^\mu \epsilon_y^\nu - 2\epsilon_z^\mu \epsilon_z^\nu), & &
\end{aligned}
\tag{A5}$$

where again  $\mu$  and  $\nu$  are the Lorentz vector indexes. Again, one may easily check that the polarization tensor components satisfy the conditions:

$$\epsilon_i^\dagger \cdot \epsilon_j = -\delta_{ij}, \quad \epsilon_{i\mu}^\mu = g_{\mu\nu} \epsilon_i^{\nu\mu} = 0, \quad P_\mu \cdot \epsilon_i^{\mu\nu} = \epsilon_{i\nu\mu} \cdot P^\mu = 0 \quad \text{for } (i, j = 1, \dots, 5). \tag{A6}$$